Iterative Synthesis of Oligoynes Capped by a $Ru_2(ap)_4$-terminus and Their Electrochemical and Optoelectronic Properties

Guo-Lin Xu,[†] Cheng-Young Wang,[‡] Yu-Hua Ni,[†] Theodore G. Goodson III,*[,‡] and Tong Ren*[,†]

Department of Chemistry, University of Miami, Coral Gables, Florida 33146, and Department of Chemistry, University of Michigan, Ann Arbor, Michigan 48109

Received March 9, 2005

Cross-coupling reactions between terminal ethynes (HC≡CY) and $Ru_2(ap)_4(C_{2(k-1)}H)$ under Hay conditions, where *ap* is 2-anilinopyridinate and $k = 2-5$, resulted in compounds $Ru_2(ap)_4(C_{2k}Y)$ (Y = Si^iPr_3 and Ph) along with the homocoupling products YC_4Y and $[Ru_2(ap)_4]_2(\mu\text{-}C_{4(k-1)})$. Compounds $Ru_2(ap)_4(C_{2k}Y)$ display two reversible Ru_2-based one-electron couples: an oxidation and a reduction. The HOMO−LUMO gaps (E_g) estimated from electrode potentials correlate linearly with the number of acetylenic bonds (k) within each series. Both nonlinear absorption and degenerate four-wave mixing measurements were carried out at both 532 and 800 nm with nano- and femtosecond laser pulses.

Introduction

Controlled syntheses of conjugated linear rod molecules have attracted immense interest during the past decade.[1,2] Linear conjugated molecules are the leading candidates for electronic and optoelectronic materials, where organic molecules have played a dominant role.[3−5] A particularly interesting group of rigid rod molecules is the family of metal compounds bearing a linear polycarbon ligand σ-bonded to either a metal center ({M}) or a metal-containing fragment, which was hailed as the new generation of organometallic materials.[6] Commonly used σ-polycarbon ligands include polyynyl[7−10] and allenylidenyl/cumulenyl,[11] as shown in Scheme 1, and the former dominates. As the prototype of molecular electronic wires, many {M}−C_{2k}−{M} type compounds of high degree of electronic mobility were reported in recent years.[12−32] Other closely related studies include multiple alkynylated ferrocenes and cyclobutadiene(cyclopentadienyl)cobalt,[33] cumulene-bridged biferrocene,[34,35] acetylide-capped linear trimetallic com-

Scheme 1. Wire-like Metalallaynes and Metalla-cumulenes

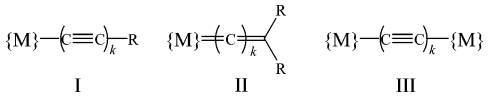

* To whom correspondence should be addressed. (T.R.) E-mail: tren@miami.edu. Tel: (305) 284-6617. Fax: (305) 284-4571. (T.G.G.) E-mail: tgoodson@umich.edu. Tel: (734) 647-0274.

† University of Miami.

‡ University of Michigan.

(1) Schwab, P. F. H.; Levin, M. D.; Michl, J. *Chem. Rev.* **1999**, *99*, 186.

(2) Manners, I. *Synthetic Metal-containing Polymers*; Wiley-VCH: Weinheim, 2004.

(3) Mullen, K.; Wegner, G. *Electronic Materials: The Oligomer Approach*; Wiley-VCH: Weinheim, 1998.

(4) Martin, R. E.; Diederich, F. *Angew. Chem., Int. Ed.* **1999**, *38*, 1350.

(5) Marks, T. J.; Ratner, M. A. *Angew. Chem., Int. Ed. Engl.* **1995**, *34*, 155.

(6) Halpern, J. *Pure Appl. Chem.* **2001**, *73*, 209.

(7) Bruce, M. I.; Low, P. J. *Adv. Organomet. Chem.* **2004**, *50*, 179.

(8) Low, P. J.; Bruce, M. I. *Adv. Organomet. Chem.* **2001**, *48*, 71.

(9) Szafert, S.; Gladysz, J. A. *Chem. Rev.* **2003**, *103*, 4175.

(10) Manna, J.; John, K. D.; Hopkins, M. D. *Adv. Organomet. Chem.* **1995**, *38*, 79.

(11) Bruce, M. I. *Chem. Rev.* **1998**, *98*, 2797.

(12) Chisholm, M. H. *Angew. Chem., Int. Ed. Engl.* **1991**, *30*, 673.

(13) Lang, H. *Angew. Chem., Int. Ed. Engl.* **1994**, *33*, 547.

(14) Bunz, U. H. F. *Angew. Chem., Int. Ed. Engl.* **1996**, *35*, 969.

(15) Paul, F.; Lapinte, C. *Coord. Chem. Rev.* **1998**, *178−180*, 431.

(16) Le Narvor, N.; Toupet, L.; Lapinte, C. *J. Am. Chem. Soc.* **1995**, *117*, 7129.

(17) Brady, M.; Weng, W.; Gladysz, J. A. *J. Chem. Soc., Chem. Commun.* **1994**, 2655.

(18) Bartik, T.; Bartik, B.; Brady, M.; Dembinski, R.; Gladysz, J. A. *Angew. Chem., Int. Ed. Engl.* **1996**, *35*, 414.

(19) Brady, M.; Weng, W.; Zou, Y.; Seyler, J. W.; Amoroso, A. J.; Arif, A. M.; Bohme, M.; Frenking, G.; Gladysz, J. A. *J. Am. Chem. Soc.* **1997**, *119*, 775.

(20) Dembinski, M.; Bartik, T.; Bartik, B.; Jaeger, M.; Gladysz, J. A. *J. Am. Chem. Soc.* **2000**, *122*, 810.

(21) Bruce, M. I.; Low, P. J.; Costuas, K.; Halet, J.-F.; Best, S. P.; Heath, G. A. *J. Am. Chem. Soc.* **2000**, *122*, 1949.

(22) Antonova, A. B.; Bruce, M. I.; Ellis, B. G.; Gaudio, M.; Humphrey, P. A.; Jevric, M.; Melino, G.; Nicholson, B. K.; Perkins, G. J.; Skelton, B. W.; Stapleton, B.; White, A. H.; Zaitseva, N. N. *Chem. Commun.* **2004**, 960.

(23) Kheradmandan, S.; Heinze, K.; Schmalle, H. W.; Berke, H. *Angew. Chem., Int. Ed.* **1999**, *38*, 2270.

(24) Fernández, F. J.; Blacque, O.; Alfonso, M.; Berke, H. *Chem. Commun.* **2001**, 1266.

(25) Fernández, F. J.; Venkatesan, K.; Blacque, O.; Alfonso, M.; Schmalle, H. W.; Berke, H. *Chem. Eur. J.* **2003**, *9*, 6192.

(26) Mohr, W.; Stahl, J.; Hampel, F.; Gladysz, J. A. *Inorg. Chem.* **2001**, *40*, 3263.

(27) Mohr, W.; Stahl, J.; Hampel, F.; Gladysz, J. A. *Chem. Eur. J.* **2003**, *9*, 3324.

(28) Stahl, J.; Bohling, J. C.; Bauer, E. B.; Peters, T. B.; Mohr, W.; Martín-Alvarez, J. M.; Hampel, F.; Gladysz, J. A. *Angew. Chem., Int. Ed.* **2002**, *41*, 1871.

(29) Horn, C. R.; Gladysz, J. A. *Eur. J. Inorg. Chem.* **2003**, 2211.

(30) Horn, C. R.; Martín-Alvarez, J. M.; Gladysz, J. A. *Organometallics* **2002**, *21*, 5386.

(31) Paul, F.; Meyer, W. E.; Toupet, L.; Jiao, H. J.; Gladysz, J. A.; Lapinte, C. *J. Am. Chem. Soc.* **2000**, *122*, 9405.

(32) Roberts, R. L.; Puschmann, H.; Howard, J. A. K.; Yamamoto, J. H.; Carty, A. J.; Low, P. J. *J. Chem. Soc., Dalton Trans.* **2003**, 1099.

(33) Bunz, U. H. F. *J. Organomet. Chem.* **2003**, *683*, 269.

(34) Skibar, W.; Kopacka, H.; Wurst, K.; Salzmann, C.; Ongania, K. H.; de Biani, F. F.; Zanello, P.; Bildstein, B. *Organometallics* **2004**, *23*, 1024.

10.1021/om050171i CCC: $30.25 © 2005 American Chemical Society
Publication on Web 05/24/2005

pounds,[36−38] metal-centered bis-allenylidene,[39] and acetylene-bridged dimers of triruthenium basic acetate.[40] Our research in this area focuses on alkynyl compounds containing diruthenium units,[41,42] and notable results include a recent demonstration of substantial charge mobility both across a Ru_2 unit between two ferrocenyl centers[43] and across carbon-rich chains between two Ru_2 centers.[44−46]

Application in nonlinear optical (NLO) materials is another active area of metal-alkynyl research.[47−49] In a broader scope, organic−inorganic hybrid materials have been a motif for nonlinear optical properties in a variety of applications.[50,51] Also, the immense interest in metal-organic nanocomposite materials has attracted interest in the fields of sensor and eye protection as well as magneto-optical effects.[52] Both second- and third-order nonlinear optical effects have been demonstrated in organometallic compounds, as they have desired characteristics such as low-energy electronic transitions and large molecular hyperpolarizabilities.[53−56]

Transition metal compounds with short polyynyl ligands are commonly obtained via the transmetalation reaction between {M}−X and M′C_{2k}Y (X = halide and M′ = Li, SnR'_3).[8,57,58] Utility of this reaction in the preparation of {M}−C_{2k}Y with $k \geq 4$ became less practical because of decreasing thermal stability of HC_{2k}Y with an increasing k. Hence, metal compounds bearing long polyynyl ligands ($C_{2(m+n)}$Y) are prepared by either the Cadiot−Chodkiewicz reaction between {M}−C_{2m}Cu and BrC_{2n}Y[59−64] or the reaction between {M}−C≡C−Au(PR_3) and XC≡CY that is driven by the elimination of XAu(PR_3) (X = halide).[65,66] More recently, Gladysz et al. demonstrated that $(C_6F_5)(p\text{-tol}_3P)_2PtC_{2k}SiEt_3$ ($k = 3-5$) can be obtained by the stepwise addition of $HCCSiEt_3$ to $(C_6F_5)(p\text{-tol}_3P)_2PtC_4H$ under Hay conditions.[26−28] Taking advantage of both the facile synthesis and aerobic stability of $Ru_2(ap)_4(C_2Y)$ and $Ru_2(ap)_4(C_4Y)$ (ap = 2-anilinopyridinate),[67−70] we elected to test the feasibility of the chain growth via the Glaser coupling reaction[60] under the conditions similar to those of Gladysz.[26−28] Reported herein are the syntheses of two $Ru_2(ap)_4(C_{2k}Y)$ series with Y as Ph and Si^iPr_3 and k = 2−5, shown in Scheme 2, and their electrochemical and nonlinear optical properties.

Scheme 2. Extended Metalallaynes $Ru_2(ap)_4(C_{2k}Y)$

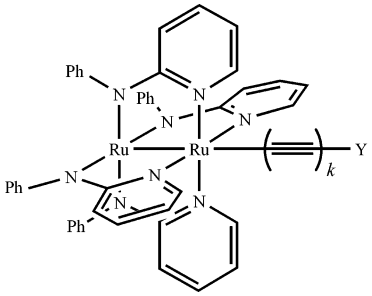

k	1	2	3	4	5
Y = Si^iPr_3	**1a**	**2a**	**3a**	**4a**	--
Y = Ph	**1b**	**2b**	**3b**	**4b**	**5b**
Y = H	**1c**	**2c**	**3c**	**4c**	--

Results and Discussion

Synthesis. Previously we demonstrated the direct synthesis of $Ru_2(ap)_4(C_4SiMe_3)$ from the reaction between $Ru_2(ap)_4Cl$ and LiC_4SiMe_3.[69] While the synthesis of $Ru_2(ap)_4(C_4Si^iPr_3)$ (**2a**) and $Ru_2(ap)_4(C_4Ph)$ (**2b**) via the same route was hampered by the lack of a commercial supply of $HC_4Si^iPr_3$ and HC_4Ph, compounds **2a** and **2b** were synthesized from the reactions between $Ru_2(ap)_4(C_2H)$ and respective HC_2Y in large excess (50−90-fold), as shown in Scheme 3. Both reactions were slow but of high yields. Obtained from treating $Ru_2(ap)_4(C_4SiMe_3)$[69] with Bu_4NF, $Ru_2(ap)_4(C_4H)$ (**2c**) underwent coupling reactions with HC_2Y (20−40 equiv) under Hay conditions at room temperature to afford the hexatriyne $Ru_2(ap)_4(C_6Y)$ (**3a/3b**) along with the homocoupling side product $Ru_2-C_8-Ru_2$. Further iteration was similarly carried out by converting $Ru_2(ap)_4(C_6Tips)$ (**3a**) to $Ru_2(ap)_4(C_6H)$ (**3c**), and the latter underwent the same cross-coupling reaction to furnish octatetrayne $Ru_2(ap)_4(C_8Y)$ (**4a/4b**).

Ideally, one would hope to reiterate the same sequence, steps (i) and (ii) in Scheme 3, many more times. However, due to the instability of compound $Ru_2(ap)_4(C_{10}Tips)$ (**5a**), attempts to isolate longer polyynes ($k \geq$

(35) Bildstein, B. *Coord. Chem. Rev.* **2000**, *126−127*, 369.
(36) Berry, J. F.; Cotton, F. A.; Murillo, C. A. *J. Chem. Soc., Dalton Trans.* **2003**, 3015.
(37) Berry, J. F.; Cotton, F. A.; Murillo, C. A.; Roberts, B. K. *Inorg. Chem.* **2004**, *43*, 2277.
(38) Berry, J. F.; Cotton, F. A.; Murillo, C. A. *Organometallics* **2004**, *23*, 2503.
(39) Rigaut, S.; Costuas, K.; Touchard, D.; Saillard, J.-Y.; Golhen, S.; Dixneuf, P. H. *J. Am. Chem. Soc.* **2004**, *126*, 4072.
(40) Chen, J. L.; Zhang, L. Y.; Chen, Z. N.; Gao, L. B.; Abe, M.; Sasaki, Y. *Inorg. Chem.* **2004**, *43*, 1481.
(41) Ren, T.; Xu, G.-L. *Comm. Inorg. Chem.* **2002**, *23*, 355.
(42) Hurst, S. K.; Ren, T. *J. Organomet. Chem.* **2003**, *670*, 188.
(43) Xu, G.-L.; DeRosa, M. C.; Crutchley, R. J.; Ren, T. *J. Am. Chem. Soc.* **2004**, *126*, 3728.
(44) Ren, T.; Zou, G.; Alvarez, J. *Chem. Commun.* **2000**, 1197.
(45) Xu, G.-L.; Zou, G.; Ni, Y.-H.; DeRosa, M. C.; Crutchley, R. J.; Ren, T. *J. Am. Chem. Soc.* **2003**, *125*, 10057.
(46) Shi, Y.; Yee, G. T.; Wang, G.; Ren, T. *J. Am. Chem. Soc.* **2004**, *126*, 10552.
(47) Whittall, I. R.; McDonagh, A. M.; Humphrey, M. G.; Samoc, M. *Adv. Organomet. Chem.* **1998**, *42*, 291.
(48) Whittall, I. R.; McDonagh, A. M.; Humphrey, M. G.; Samoc, M. *Adv. Organomet. Chem.* **1999**, *43*, 349.
(49) Coe, B. J.; Curati, N. R. M. *Comm. Inorg. Chem.* **2004**, *25*, 147.
(50) *Optoelectronic Properties of Inorganic Compounds*; Roundhill, D. M.; Fackler, J. P., Ed.; Plenum Press: New York, 1999.
(51) Goodson, T. G. *Acc. Chem. Res.* **2005**, *37*, 99.
(52) Ispasoiu, R. G.; Balogh, L.; Varnavski, O. P.; Tomalia, D. A.; Goodson, T. *J. Am. Chem. Soc.* **2000**, *122*, 11005.
(53) Nalwa, H. S. *Appl. Organomet. Chem.* **1991**, *5*, 349.
(54) Zhai, T.; Lawson, C. M.; Burgess, G. E.; Lewis, M. L.; Gale, D. C.; Gray, G. M. *Opt. Lett.* **1994**, *19*, 871.
(55) Ando, M.; Kadono, K.; Haruta, M.; Sakaguchi, T.; Miya, M. *Nature* **1995**, *374*, 625.
(56) Kanis, D. R.; Ratner, M. A.; Marks, T. J. *J. Am. Chem. Soc.* **1992**, *114*, 10338.
(57) *Modern Acetylene Chemistry*; Stang, P. J.; Diederich, F., Ed.; VCH: Weinheim, 1995.
(58) *Acetylene Chemistry: Chemistry, Biology and Materials Science*; Diederich, F.; Tykwinski, R. R.; Stang, P. J., Eds.; Wiley-VCH: Weinheim, 2004.
(59) Brandsma, L. *Preparative Acetylenic Chemistry*; Elsevier: Amsterdam, 1988.
(60) Siemsen, P.; Livingston, R. C.; Diederich, F. *Angew. Chem., Int. Ed.* **2000**, *39*, 2632.
(61) Dembinski, R.; Lis, T.; Szafert, S.; Mayne, C. L.; Bartik, T.; Gladysz, J. A. *J. Organomet. Chem.* **1999**, *578*, 229.
(62) Yam, V. W.-W.; Chong, S. H.-F.; Ko, C.-C.; Cheung, K.-K. *Organometallics* **2000**, *19*, 5092.
(63) Yam, V. W. W. *J. Organomet. Chem.* **2004**, *689*, 1393.
(64) Bruce, M. I.; Kramarczuk, K. A.; Zaitseva, N. N.; Skelton, B. W.; White, A. H. *J. Organomet. Chem.* **2005**, *690*, 1549.
(65) Bruce, M. I.; Skelton, B. W.; White, A. H.; Zaitseva, N. N. *J. Organomet. Chem.* **2003**, *683*, 398.
(66) Bruce, M. I.; Humphrey, P. A.; Melino, G.; Skelton, B. W.; White, A. H.; Zaitseva, N. N. *Inorg. Chim. Acta* **2005**, *358*, 1453.
(67) Chakravarty, A. R.; Cotton, F. A. *Inorg. Chim. Acta* **1986**, *113*, 19.
(68) Zou, G.; Alvarez, J. C.; Ren, T. *J. Organomet. Chem.* **2000**, *596*, 152.
(69) Xu, G.; Ren, T. *Organometallics* **2001**, *20*, 2400.
(70) Ren, T. *Organometallics* **2002**, *21*, 732.

Table 1. Yields of Ru_2-Containing Products from Glaser Coupling Reactions

k	**2**	**3**	**4**	**5**
Y = Si^iPr_3	**2a** (67%)	**3a** (51%) $Ru_2-C_8-Ru_2$ (40%)	**4a** (23%) $Ru_2-C_{12}-Ru_2$ (60%)	
Y = Ph	**2b** (81%)	**3b** (54%) $Ru_2-C_8-Ru_2$ (30%)	**4b** (51%) $Ru_2-C_{12}-Ru_2$ (35%)	**5b** (36%[a]) $Ru_2-C_{16}-Ru_2$[b]

[a] The yield of compound **5b** was calculated based on **3c**. [b] Detected in MOLDI-MS, but yield undetermined.

Scheme 3. Synthesis of $Ru_2(ap)4(C_{2k}Y)$ ($Ru_2(ap)4 = Ru_2$)[a]

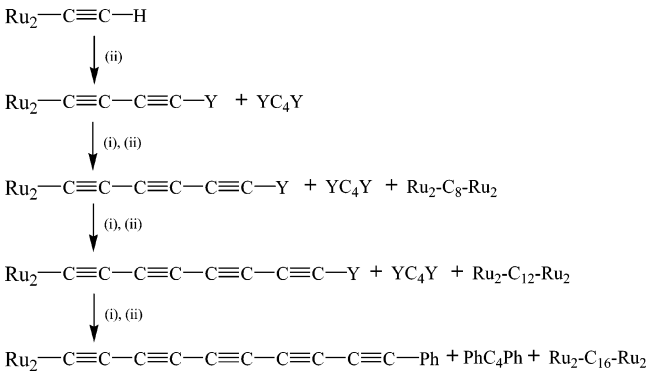

[a] (i) Y = Si^iPr_3, Bu_4NF; (ii) HC_2Y (Y = Si^iPr_3 or Ph), CuCl, TMEDA, O_2, room temperature.

5) failed. When **4c** was used as the starting material, the resultant decapentayne **5a** was desilylated in situ (probably by either TMEDA or OH^-(aq)) and hence could not be isolated. Nevertheless, the phenyl-capped decapentayne **5b** was isolated in a reasonable yield from a reaction sequence starting from **3c** to yield **4a**, converting the latter to **4c** without purification for the following step to yield **5b** (see Experimental Section). Compounds **2**−**5** were all purified via the extraction and subsequent column chromatography, and their yields are listed in Table 1. Similar to the ethynyl compounds (**1**),[67,68,70] compounds **2**−**5** are $S = 3/2$ paramagnetic species with μ_{eff} ranging from 3.7 to 4.10 μ_B. The compositions of **2**−**5** have been ascertained through both the observation of corresponding molecular ions in FAB-MS and satisfactory combustion analysis.

Despite the presence of HC_2Y in large excess as the sacrificial reactant, compounds $Ru_2-C_{4k}-Ru_2$ were always present (yields also listed in Table 1) as the byproducts with $k = 2-4$, indicating the propensity for homocoupling of $Ru_2(ap)_4(C_{2k}H)$ type compounds. Compounds $Ru_2-C_{4k}-Ru_2$ are known[44,45] and were identified through the comparison of the R_f values with the authentic compounds. Similarly, byproduct $(C_6F_5)(p\text{-}tol_3P)_2Pt\text{-}(\mu\text{-}C_{4(k-1)})\text{-}Pt(C_6F_5)(p\text{-}tol_3P)_2$ was isolated in a significant yield (ca. 25%) in the aforementioned preparation of $(C_6F_5)(p\text{-}tol_3P)_2PtC_{2k}SiEt_3$ ($k = 3$ and 4).[27] Interestingly, the attempt to prepare $(C_6F_5)(p\text{-}tol_3P)_2PtC_{10}SiEt_3$ yielded $(C_6F_5)(p\text{-}tol_3P)_2Pt\text{-}(\mu\text{-}C_{16})\text{-}Pt(C_6F_5)(p\text{-}tol_3P)_2$ as the main product along with trace amounts of $(C_6F_5)(p\text{-}tol_3P)_2Pt\text{-}(\mu\text{-}C_{20})\text{-}Pt(C_6F_5)(p\text{-}tol_3P)_2$ and $(C_6F_5)(p\text{-}tol_3P)_2Pt\text{-}(\mu\text{-}C_{24})\text{-}Pt(C_6F_5)(p\text{-}tol_3P)_2$.[27] This is in agreement with our observation that $[M]-C_{2k}SiR_3$ ($k = 4$ and 5) is desilylated in situ and undergoes facile homocoupling.

An observation unique to the present study is the absence of $Ru_2-C_4-Ru_2$ from the reactions involving $Ru_2(ap)_4(C_2H)$. This observation corroborates the long-standing speculation that a dicopper species (**6** in Scheme 4) is the key intermediate in a Glaser coupling reaction.[60] The homocoupling of $Ru_2(ap)_4(C_2H)$ would require the placement of two $Ru_2(ap)_4$ units immediately adjacent to the dicopper core in **6**, which is prohibited by the bulkiness of $Ru_2(ap)_4$. The success of the cross coupling between $Ru_2(ap)_4(C_2H)$ and organic ethynes, however, clearly indicates that the incorporation of single $Ru_2(ap)_4(C_2H)$ in **6** is feasible. The potential steric crowding is significantly reduced with $k \geq 2$, and consequently the homocoupling of $Ru_2(ap)_4(C_{2k}H)$ becomes a competitive pathway.

Scheme 4. Dicopper Intermediates 6 in Glaser Coupling Reaction[a]

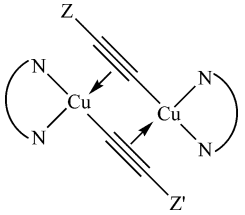

[a] Z and Z′ are ethynyl substituents.

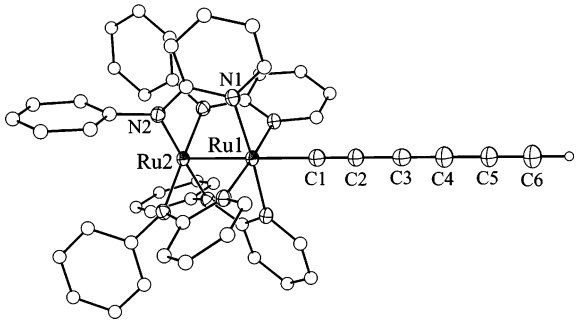

Figure 1. ORTEP plot of compound **3c** at 30% probability level. All hydrogen atoms except the acetylenic hydrogen were omitted for clarity. Selected bond lengths (Å) and angles (deg): Ru1−Ru2, 2.3279(6); Ru1−N1, 2.090(4); Ru2−N2, 2.035(3); Ru1−C1, 2.082(8); C1−C2, 1.207(11); C2−C3, 1.389(11); C3−C4, 1.249(14); C4−C5, 1.277(15); C5−C6, 1.200(12); N1−Ru1−Ru2, 87.86(11); N2−Ru2−Ru1, 89.34(10); N1−Ru1−Ru2−N2, 17.59(13).

Molecular Structure of $Ru_2(ap)_4(C_6H)$. Although most $Ru_2(ap)_4(C_{2k}Y)$ compounds reported herein are microcrystalline as synthesized, $Ru_2(ap)_4(C_6H)$ (**3c**) was the only compound successfully crystallized. The molecular structure of **3c** is shown in Figure 1, along with some selected bond lengths and angles. Crystallized in the *P*4*nc* space group, molecule **3c** contains a crystallographic 4-fold axis that coincides with the Ru_2-C_6H vector, which enforces a collinear geometry of the nine-atom chain −Ru2−Ru1−C1−C2−C3−C4−C5−C6−H6. Crystallographically characterized σ-hexatriynyl complexes include $Cp^*Re(NO)(PPh_3)(C_6Ph)$,[61] $Re(CO)_3(bipy)(C_6Y)$ (Y = Ph and $SiMe_3$),[62] $(C_6F_5)(p\text{-}tol_3P)_2PtC_6Y$ (Y = $SiEt_3$ and $CMe_2(OSiEt_3)$), and $(p\text{-tolyl})(p\text{-}tol_3P)_2PtC_6SiEt_3$,[71] where the hexatriynyl chain was always slightly curved. It is clear from Figure 1 that the coordination

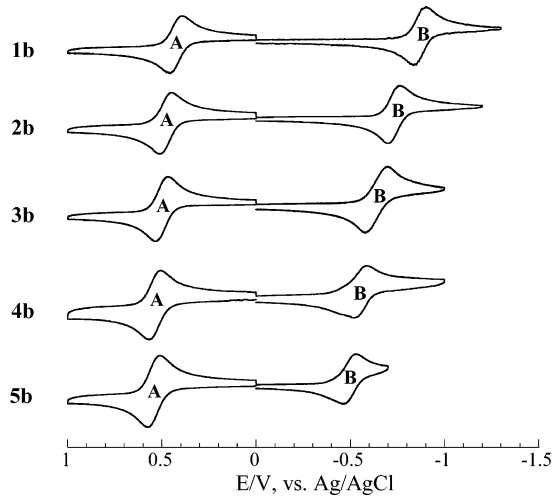

Figure 2. Cyclic voltammograms of $Ru_2(ap)_4(C_{2k}Ph)$ recorded vs Ag/AgCl in 0.20 M THF solution of Bu_4NPF_6 at a scan rate of 0.10 V/s.

environment of the Ru2(II,III) core in **3c** resembles those found for $Ru_2(ap)_4(C_2Y)$ type compounds in previous studies.[70] The *ap* ligands adopt the (4,0) arrangement with all anilino N-centers coordinated to the Ru2 center (*4* site) and all pyridine N-centers coordinated to the Ru1 center (*0* site), which is also σ-bonded to the hexatriynyl fragment. The Ru−Ru (2.3279(6) Å) and Ru−C_α (2.082(8)Å) bond lengths in **3c** are about the same as those in the previously reported compounds $Ru_2(ap)_4(C_2Y)$ (ca. 2.33 Å for Ru−Ru and 2.07 Å for Ru−C_α bonds, respectively). It is noteworthy that while two of three acetylene bonds (C1−C2 and C5−C6) are of normal distances, the other, C3−C4, is quite long, and the adjacent C4−C5 is short for a C−C single bond.[9] The abnormality is unlikely a crystallographic artifact since the structure was refined with a data set of high 2θ angle (70° with Mo Kα) to excellent figures of merit.

Electrochemistry. Rich redox chemistry has been the hallmark of diruthenium alkynyl compounds, and $Ru_2(ap)_4(C_{2k}Y)$ type compounds are no exceptions. As shown in the cyclic voltammograms recorded for $Ru_2(ap)_4(C_{2k}Ph)$ (Figure 2), compounds **1**−**5** generally display two one-electron couples: an oxidation (**A**) and a reduction (**B**), and both are localized on the Ru_2 centers, as demonstrated in the earlier studies of $Ru_2(ap)_4(C_2Y)$ type compounds.[67−70] While the oxidation couple **A** is reversible throughout the series, the reduction couple **B** becomes less reversible with concurrent loss of both i_{pa} and i_{pc} as the number of acetylene bonds (k) increases. Similar variation was also observed for the $Ru_2(ap)_4(C_{2k}Si^iPr_3)$ series, the CVs of which are provided in the Supporting Information. Electrode potentials from the CVs measured for compounds **1**−**5** are listed in Table 2 along with some related parameters.

It is clear from Table 2 that the $E_{1/2}$ of both couples **A** and **B** of $Ru_2(ap)_4(C_{2k}Ph)$ shift anodically as k increases, but with different increments: $E_{1/2}$(**B**) increases ca. 95 mV per C≡C bond, while $E_{1/2}$(**A**) increases only ca. 25 mV. The same trends are observed for compounds $Ru_2(ap)_4(C_{2k}Si^iPr_3)$ with the potential increment per C≡C bond ca. 105 mV for $E_{1/2}$(**B**) and ca. 22 mV for $E_{1/2}$(**A**). The general trend of the anodic shift in $E_{1/2}$ as k increases is easily understood: the acetylene unit is electron-deficient and strongly electron-withdrawing.

Consequently, the more acetylene units, the harder to oxidize and easier to reduce $Ru_2(ap)_4(C_{2k}Y)$. Although the exact rationale for the difference in the magnitude of potential shifts between couples **A** and **B** should await MO analysis based on first-principle calculations, one can hypothesize that the LUMO of $Ru_2(ap)_4(C_{2k}Y)$ is more sensitive to the nature of polyynyl than the HOMO. Prior theoretical analysis of *mononuclear* metal-alkynyl complexes revealed that (i) the HOMO often contains the filled−filled d_π−π(C≡C) interaction that is repulsive in nature and (ii) π^*(C≡C) lies high above both the HOMO and LUMO in general.[72−74] The one-electron oxidation of $Ru_2(ap)_4(C_2R)$ removes one of the d_π electrons, which reduces the repulsion between d_π and π(C≡C) orbitals and facilitates a limited dependence on the polyynyl chain length. On the other hand, the one-electron reduction on the Ru_2-core will greatly elevate the energy of the d_π orbital, which results in a much improved overlap between $d_\pi(Ru_2)$ and π^*(C≡C) and hence the extensive delocalization of the added electron. Consequently, the electrode potential of **B** is far more sensitive to the polyynyl chain length than that of **A**.

Spectral Properties. Compounds $Ru_2(ap)_4(C_{2k}Y)$ generally display two intense bands in the visible−near-infrared (vis−NIR) region centered at ca. 470 and 760 nm, and spectra of compounds **1b**−**5b** are shown in Figure 3. The low-energy band is assigned to the $\delta(Ru_2) \rightarrow \delta^*(Ru_2)$ transition that is largely localized on the $Ru_2(ap)_4$ core, and the λ_{max} (Table 2) gradually red-shifts as the polyynyl elongates, albeit the magnitude of the shift per C≡C unit is very small. The high-energy band at ca. 470 nm is attributed to the $\pi(N) \rightarrow \pi^*(Ru_2)$ transition, and the latter orbital contains a possibly significant contribution from a π^*(C≡C) orbital.[45] The broad nature of the spectral envelope of high-energy transition implies the possibility of multiple transitions in this region, which may be responsible for the lack of the dependence of λ_{max} on polyynyl length. The optical transition energies estimated from the λ_{max} of both bands are listed in Table 2 for compounds **1**−**5**. Obviously, the optical gap (the smaller E_{op}) is consistently larger than the electrochemical E_g across both series. Detailed spectroscopic analysis of other Ru2(II,III) compounds, primarily the $Ru_2(O_2CR)_4Cl$ family, revealed the pseudodegeneracy of $\pi^*(Ru_2)$ and $\delta^*(Ru_2)$ orbitals, which results in an ensemble of low-energy excited states.[75] The lowest dipole-allowed transition in $Ru_2(ap)_4(C_{2k}Y)$ probably involves a virtual orbital other than the LUMO, which leads to the discrepancy between E_{op} and E_g.

The extent of π-conjugation in linear oligomers is a key measure of their potential as electrophores/chro-

(71) Mohr, W.; Peters, T. B.; Bohling, J. C.; Hampel, F.; Arif, A. M.; Gladysz, J. A. *C. R. Chim.* **2002**, *5*, 111.

(72) Lichtenberger, D. L.; Renshaw, S. K.; Bullock, R. M. *J. Am. Chem. Soc.* **1993**, *115*, 3276.

(73) Lichtenberger, D. L.; Renshaw, S. K.; Wong, A.; Tagge, C. D. *Organometallics* **1993**, *12*, 3522.

(74) Koentjoro, O. F.; Rousseau, R.; Low, P. J. *Organometallics* **2001**, *20*, 4502.

(75) Miskowski, V. M.; Hopkins, M. D.; Winkler, J. R.; Gray, H. B. In *Inorganic Electronic Structure and Spectroscopy*; Solomon,E. I.; Lever, A. B. P., Eds.; Wiley: New York, 1999; Vol. 2; p 343.

Table 2. Electrode Potentials and Spectral Data for Compounds 1−5

	$E_{1/2}$(**A**)/V (ΔE_p/V, $i_{backward}/i_{forward}$)	$E_{1/2}$(**B**)/V (ΔE_p/V, $i_{backward}/i_{forward}$)	E_g/V[a]	E_{op}, eV[b] (λ_{max}, nm)
1a[c]	0.455 (0.103, 0.99)	−0.877 (0.109, 0.96)	1.332	1.67 (745) 2.64 (471)
2a	0.491 (0.066, 0.97)	−0.740 (0.061, 0.87)	1.231	1.63 (761) 2.51 (494)
3a	0.514 (0.063, 0.98)	−0.622 (0.067, 0.98)	1.136	1.62 (767) 2.60 (477)
4a	0.536 (0.057, 0.97)	−0.561 (0.063, 0.89)	1.097	1.61 (773) 2.61 (476)
1b[d]	0.439 (0.066, 0.96)	−0.877 (0.069, 0.95)	1.316	1.65 (751) 2.59 (479)
2b	0.482 (0.059, 0.94)	−0.736 (0.060, 0.97)	1.218	1.63 (761) 2.55 (487)
3b	0.497 (0.062, 0.99)	−0.647 (0.070, 0.95)	1.144	1.62 (766) 2.70 (460)
4b	0.538 (0.064, 0.98)	−0.553 (0.068, 0.99)	1.091	1.61 (772) 2.64 (456, 485)
5b	0.543 (0.062, 0.99)	−0.495 (0.073, 0.69)	1.038	1.59 (779) 2.47 (502)

[a] $E_g(V) = E_{1/2}(0/+1) - E_{1/2}(0/-1)$. [b] $E_{op}(eV) = 1240/\lambda$. [c] Data taken from ref 65. [d] Previously published data were obtained from solvents other than THF; data listed here were remeasured under the same conditions as that used for other compounds reported in this contribution.

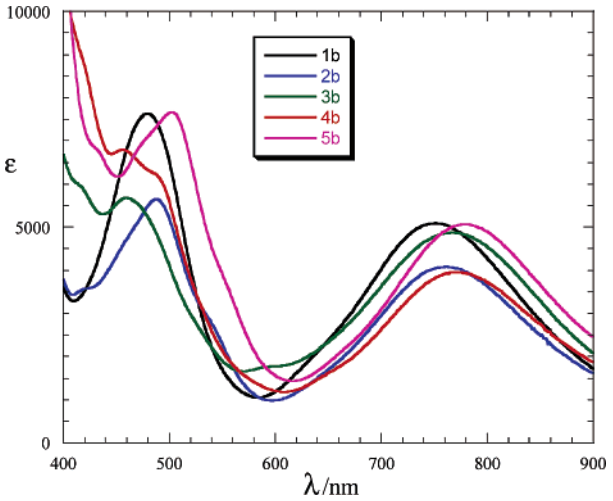

Figure 3. Vis−NIR spectra recorded in THF for compounds **1b**−**5b**.

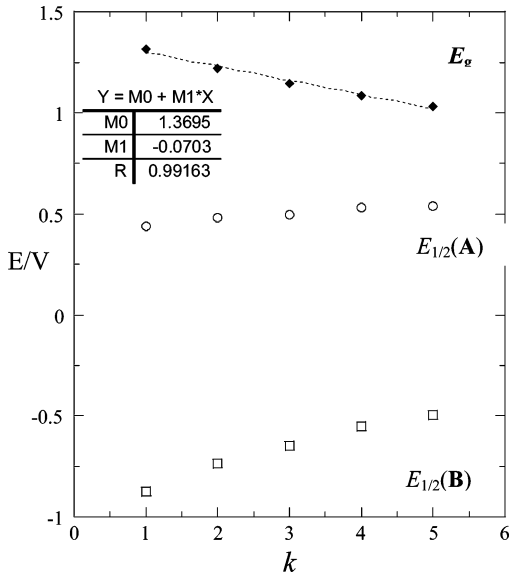

Figure 4. Plots of $E_{1/2}$(**A**) (circles), $E_{1/2}$(**B**) (squares), and E_g (diamonds) vs k for compounds $Ru_2(ap)_4(C_{2k}Ph)$.

mophores[3] and is commonly gauged through a linear correlation between the lowest optical gap (E_{op}) and reciprocal chain length ($1/k$).[4,76] Such E_{op} vs $1/k$ plots have been demonstrated in oligoynes bearing both organic and organometallic capping groups, such as benzyl ether dendrons by Hirsch et al.,[77] phosphine-Au(I) complexes by Che et al.,[78] and the aforementioned $(PAr_3)_2(C_6F_5)$Pt cap by Gladysz et al.[27] In each of these cases, the transition on the basis of which the E_{op} was calculated is attributed to $\pi(C{\equiv}C) \rightarrow \pi^*(C{\equiv}C)$. In the case of Ru_2-oligoynes $Ru_2(ap)_4(C_{2k}Y)$, the HOMO−LUMO gap can be estimated from electrode potentials: $E_g = E_{1/2}(A) - E_{1/2}(B)$ (Table 2).[79,80] However, the E_g−$(1/k)$ plot is surprisingly nonlinear. Instead, the E_g−k plot is clearly linear (correlation coefficient $R = 99.2\%$) for compounds **1b**−**5b**, as shown in Figure 4. The similar linear relationships can also be obtained for the **1a**−**4a** series (Supporting Information). These linear relationships derived from voltammetric measurements appear to indicate that the conjugation along the Ru_2−oligoyne linkage is extensive.

To further gauge the degree of electronic delocalization, the third-order NLO responses of compounds **1b**−**5b** were measured using both nonlinear transmission and degenerate four-wave mixing (DFWM) measurements.[81] Shown in Table 3 are the values for the third-order NLO effect at both 532 and 800 nm. At 800 nm, most of the compounds (**1b**−**5b**) yielded third-order susceptibilities (imaginary part, $Im\chi^{(3)}$) on the order of 1×10^{-8} esu. The absence of a significant dependence of the NLO susceptibility on the chain length (k) at 800 nm is understandable since the excitation ($\delta(Ru_2) \rightarrow \delta^*(Ru_2)$) is localized on the Ru_2 core and does not involve the oligoynyl chain.

Shown in Figure 5 is the result of four-wave-mixing measurements of compound **3b** at 532 nm and nano-

(76) Meier, H.; Stalmach, U.; Krishorn, H. *Acta Polym.* **1997**, *48*, 379.
(77) Gibtner, T.; Hampel, F.; Gisselbrecht, J.-P.; Hirsch, A. *Chem. Eur. J.* **2002**, *8*, 408.
(78) Lu, W.; Xiang, H.-F.; Zhu, N.; Che, C.-M. *Organometallics* **2002**, *21*, 2343.
(79) Ren, T. *Coord. Chem. Rev.* **1998**, *175*, 43.
(80) Loutfy, R. O.; Loutfy, R. O. *Can. J. Chem.* **1976**, *54*, 1454.

(81) The DFWM apparatus has been described in the literature.

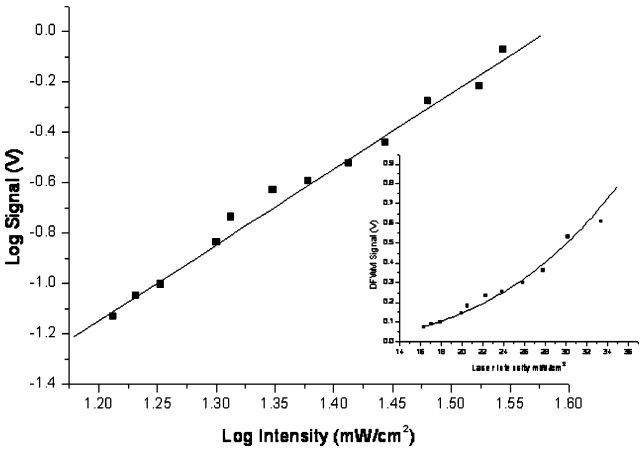

Figure 5. Intensity dependence of the DFWM signal for compound **3b**.

Table 3. Third-Order Nonlinear Optical Susceptibilities of Compounds 1b−5b, $\chi^{(3)}$/C (10^{-8} esu M^{-1}), Measured at 800 and 532 nm

compound (k)	800 nm	532 nm
1b (1)		2.70 ± 0.41
2b (2)	1.02 ± 0.15	3.97 ± 0.6
3b (3)	1.52 ± 0.23	15.0 ± 2.3
4b (4)	1.02 ± 0.15	6.08 ± 0.92
5b (5)	1.48 ± 0.22	10.9 ± 1.6

second pulses. Here the log of the intensity of the signal beam is plotted as a function of the log of the incident intensity (measured in GW/cm^2). The log−log plot shows a linear dependence with a slope of 3. The inset in Figure 5 shows the cubic dependence more closely. Similar measurements with the other members of the series (**1b**, **2b**, **4b**, and **5b**) were carried out. From the intercept of the intensity dependence curves the magnitude of the nonlinear effect was estimated for each sample. With the use of CS_2 as a standard, the values of the resonant third-order susceptibility were then calculated and tabulated in Table 3 for compounds **1b**−**5b**. In an attempt to account for resonance enhancement of the sample near 532 nm, corrections of the nonlinear effect were carried out (see eq 1 in Experimental Section below). However, it should be clear that in this comparison the absolute value is not as critical as the relative value of the Ru complexes as a function of k. While it is difficult to accurately calculate the electronic $\chi^{(3)}$ when the DFWM signal is measured in the resonance of the linear absorption (and due to the relatively broad absorption bands which may be overlapped), there was an increasingly large value obtained for the susceptibility (up to a value of 1.83×10^{-19} M^2/V^2). The resonant $\chi^{(3)}$ values of the compounds **1b**−**5b** are much higher than that of polyacetylenes, ca. 1.0×10^{-14} esu (1.396×10^{-22} M^2/V^2), measured using DFWM at 532 nm.[82]

The trend in the DFWM results for the different conjugated chain lengths is interesting for the purpose of enhancing the NLO effect. Recent work by Coe et al. described a chain length dependence in the measured molecular hyperpolarizability for a series of donor (Ru^{II} complex)−acceptor (methylpyridinium) pairs linked by oligoene bridge.[83−85] Within each set of the Ru-donor−acceptor motifs of varying lengths of the oligoene chain, it was found that the molecular hyperpolarizability decreased as a function of increasing chain length. This is quite surprising, as the previous reports had suggested an increase in molecular hyperpolarizability with an increase in conjugation length. For instance, the recent measurement of the second-order molecular hyperpolarizability (γ) of triisopropylsilyl (Tips)-capped oligoynes, namely, Tips−C_{2n}−Tips with $n = 2-10$, revealed a substantial increase in γ as the chain length increases (power law determined: $\gamma \sim n^{4.28}$).[86,87] Molecular orbital considerations were used by Coe et al. to explain this seemingly contradiction to the normal design criteria for improved nonlinear optical materials after reaching a limit of conjugation length. Specifically, it was found that the HOMO gains in π-character as one proceeds through the series of compounds. This leads to a significant degree of ILCT character in the lowest energy transition as the chain length is increased. This may be the reason there is a limit to the effect of the chain extension on the molecular hyperpolarizability. Clearly, the tuning of the HOMO−LUMO gap as reflected by the voltammetric data herein and by absorption data from the work of Coe et al.[83−85] may not be the only determining factor in describing the dependence of molecular hyperpolarizabilities on conjugation length in organometallic compounds.

Conclusion

We demonstrated that (i) [Ru_2]-caped oligoynes can be obtained using the Glaser coupling reaction; (ii) the electrochemical HOMO−LUMO gaps (E_g) of metallo-oligoyne correlate linearly with the number of triple bonds; and (iii) [Ru_2]-caped oligoynes exhibit significant third-order NLO susceptibilities in the visible region with nanosecond pulses. However, the tuning of E_g by varying the number of C≡C bonds did not result in a monotonic increase in $\chi^{(3)}$ beyond $k = 3$. The lack of simple structure−property relationships in Ru_2-alkynyl compounds is being further examined both theoretically and synthetically.

Experimental Section

Triisopropylsilylacetylene, 1,4-bis(trimethylsilyl)-1,3-butadiyne, 2-anilinopyridine, and n-BuLi were purchased from Aldrich, phenylacetylene, Bu_4NF in THF, CuCl, and TMEDA were from ACROS, and silica gel was from Merck. $Ru_2(ap)_4(C_2Si^iPr_3)$ (**1a**),[70] $Ru_2(ap)_4(C_2Ph)$ (**1b**),[67] $Ru_2(ap)_4(C_2H)$ (**1c**),[55] and $Ru_2(ap)_4(C_4SiMe_3)$[56] were prepared according to literature procedures. THF was distilled over Na/benzophenone under an N_2 atmosphere prior to use. Infrared spectra were recorded on Perkin-Elmer 2000 FT-IR spectrometer using KBr disks. UV−vis spectral data were acquired in THF solution using a

(82) Dorsinville, R.; Yang, L.; Alfano, R. R.; Tubino, R.; Destri, S. *Solid State Commun.* **1988**, *68*, 875.

(83) Coe, B. J.; Jones, L. A.; Harris, J. A.; Brunschwig, B. S.; Asselberghs, I.; Clays, K.; Persoons, A. *J. Am. Chem. Soc.* **2003**, *125*, 862.

(84) Coe, B. J.; Jones, L. A.; Harris, J. A.; Brunschwig, B. S.; Asselberghs, I.; Clays, K.; Persoons, A.; Garín, J.; Orduna, J. *J. Am. Chem. Soc.* **2004**, *126*, 3880.

(85) Coe, B. J.; Harris, J. A.; Brunschwig, B. S.; Garín, J.; Orduna, J.; Coles, S. J.; Hursthouse, M. B. *J. Am. Chem. Soc.* **2004**, *126*, 10418.

(86) Slepkov, A. D.; Hegmann, F. A.; Eisler, S.; Elliott, E.; Tykwinski, R. R. *J. Chem. Phys.* **2004**, *120*, 6807.

(87) Eisler, S.; Slepkov, A. D.; Erin Elliott, T. L.; McDonald, R.; Hegmann, F. A.; Tykwinski, R. R. *J. Am. Chem. Soc.* **2005**, *127*, 2666.

Perkin-Elmer Lambda900 UV/vis/NIR spectrophotometer. Magnetic susceptibility was measured with a Johnson Matthey MarkII magnetic susceptibility balance at 294 ± 2 K. Cyclic voltammograms were recorded on a CHI620A voltammetric analyzer with a glassy carbon working electrode, a Pt wire auxiliary electrode, and a Ag/AgCl reference electrode in 0.2 M *n*-Bu_4NPF_6 in THF. The ferrocenium/ferrocene couple was observed at 0.564 V at the experimental conditions.

Preparation of $Ru_2(ap)_4(C_4H)$ (2c). To a THF solution of 1.02 g (1.0 mmol) of $Ru_2(ap)_4(C_4SiMe_3)$ was added 0.50 mL of Bu_4NF (1.0 M solution in THF), and the mixture was stirred for 10 min. After the removal of THF, the residue was washed with copious amount of methanol and the solid was collected by filtration and dried under vacuum. Yield: 0.87 g (94%).

Preparation of $Ru_2(ap)_4(C_4Y)$ (Y = Si^iPr_3 (2a) and Ph (2b)). A three-neck flask equipped with an additional funnel was charged with 40 mL of THF, compound **1c** (0.30 mmol), CuCl (20 mg), and TMEDA (0.1 mL). Phenylacetylene (27.3 mmol, 3.0 mL in 40 mL of THF) was added to the reaction mixture at the rate of 5 mL/h, while air was gently bubbled through the solution. The reaction was complete in 10 h, as indicated by the disappearance of **1c** on TLC. After the removal of solvents, the residue was washed with copious amount of methanol and then purified on silica column. Yield of **2b**: 0.245 g (81.3% based on Ru). Data for **2b**: R_f, 0.40 (hexanes/ethyl acetate/triethylamine, 10:1:1, v/v, the same combination is also used for the determination of other R_f's). Anal. for $C_{54}H_{41}N_8Ru_2 \cdot C_4H_8O_2$ Found (Calc): C, 63.44 (63.78); H, 4.77 (4.52); N, 10.37 (10.26). MS-FAB (*m/e*, based on ^{101}Ru): 1004 [M^+]. UV−vis data, λ_{max} (nm, ϵ(M^{-1} cm^{-1})): 758(5600), 487(7790). ν(C≡C) (cm^{-1}, KBr disk): 2164 (w). χ_g, 5.18 × 10^{-6} emu, μ_{eff}, 3.73 μ_B.

Compound **2a** was similarly prepared from the reaction between 0.272 g of **1c** and 40 mL of 1.0 M $HCCSi^iPr_3$ in THF over a period of 4 h, and the yield was 54% based on Ru. TLC also indicated the formation of a significant amount of $Ru_2(ap)_4Cl$. Data for **2a**: R_f, 0.69. Anal. Found (Calc) for $C_{57}H_{57}N_8SiRu_2 \cdot 1/2CH_2Cl_2$: C, 61.80 (61.74); H, 5.34 (5.53); N, 9.90 (9.68). MS-FAB (*m/e*, based on ^{101}Ru): 1084 [M^+]. UV−vis data, λ_{max} (nm, ϵ(M^{-1} cm^{-1})): 761(4320), 479(5940); ν(C≡C) (cm^{-1}, KBr disk): 2141 (w), 2108 (w). χ_g, 5.03 × 10^{-6} emu, μ_{eff}, 3.85 μ_B.

Preparation of $Ru_2(ap)_4(C_6Y)$ (Y = Si^iPr_3 (3a) and Ph (3b)). To a 50 mL THF solution containing 0.185 g of $Ru_2(ap)_4(C_4H)$ (**2c**) (0.20 mmol) was added 4.0 mL of 1.0 M HC_2Ph in THF, 0.10 mL of TMEDA, and 20 mg of CuCl. Air was gently bubbled through the solution, and the reaction was terminated upon the disappearance of **2c** (2 h) as indicated by TLC. After the solvent removal, compound **3b** was extracted from the residue using 100 mL of acetone. The crude extract was further purified by column chromatography using a linear gradient of eluents (hexanes/ethyl acetate/triethylamine, 95:0:5−85:10:5, v/v) to yield **3b** as a brown crystalline material (0.11 g, 54%). The residue after acetone extraction was purified by repeated washing of methanol and water and subsequent recrystallization from CH_3OH/toluene and identified as [$Ru_2(ap)_4$](μ-C_8) by FAB-MS. Synthesis of **3a** is the same as that of **3b** except HC_2Tips was used instead of HC_2Ph and the reaction was also complete in 2 h. Yield: 51%.

Data for **3a**: R_f, 0.62. Anal. Found (Calc) for $C_{59}H_{57}N_8SiRu_2$: C, 63.74 (63.96); H, 5.33 (5.15); N, 9.96 (10.12). MS-FAB (*m/e*, based on ^{101}Ru): 1108 [M^+]. UV−vis data, λ_{max} (nm, ϵ(M^{-1} cm^{-1})): 767(8830), 477(10900). ν(C≡C) (cm^{-1}, KBr disk): 2140(w), 1966(w). χ_g, 5.15 × 10^{-6} emu, μ_{eff}, 3.89 μ_B.

Data for **3b**: R_f, 0.38. Anal. Found (Calc) for $C_{56}H_{41}N_8Ru_2 \cdot 3H_2O$: C, 62.40 (62.16); H, 4.47 (4.35); N, 10.19 (10.36). MS-FAB (*m/e*, based on ^{101}Ru): 1028 [M^+]. UV−vis data, λ_{max} (nm, ϵ($M^{-1}cm^{-1}$)): 768(5330) and 471(7660). ν(C≡C) (cm^{-1}, KBr disk): 2115(w), 1975(w). χ_g, 6.26 × 10^{-6} emu, μ_{eff}, 4.05 μ_B.

Preparation of $Ru_2(ap)_4(C_6H)$ (3c). To a THF/CH_3OH (3:1, v/v) solution of 0.55 g (0.50 mmol) of $Ru_2(ap)_4(C_6Si^iPr_3)$ was added K_2CO_3 (0.70 g), and the mixture was stirred for 2 h. The reaction mixture was filtered, and the filtrate was dried under vacuum. The residue was washed with copious amount of methanol, and the solid was collected by filtration, dried under vacuum, and subjected to the coupling reactions without further purification.

Preparation of $Ru_2(ap)_4(C_8Y)$ (Y = Si^iPr_3 (4a) and Ph (4b)). To a 40 mL THF solution containing 0.200 g of $Ru_2(ap)_4(C_6H)$ (**3c**) (0.21 mmol) was added 2.0 mL of 1.0 M HC_2Ph in THF, 0.10 mL of TMEDA, and 20 mg of CuCl. Air was gently bubbled through the solution, and the reaction was terminated upon the disappearance of **3c** (∼0.5 h), as indicated by TLC. After the solvent removal, compound **4b** was extracted from the residue using 100 mL of acetone. The crude extract was further purified by column chromatography using a linear solvent gradient (hexanes/ethyl acetate/triethylamine, 95:0:5−85:10:5, v/v) to yield **4b** as a brown crystalline material (0.113 g, 51%). Synthesis of **4a** is similar to that of **4b** except HC_2Tips was used instead of HC_2Ph, and the reaction was complete within 30 min. Yield: 23%. Data for **4a**: R_f, 0.64. Anal. Found (Calc) for $C_{61}H_{57}N_8SiRu_2 \cdot H_2O$: C, 63.84 (63.71); H, 5.19 (5.13); N, 9.47 (9.75). MS-FAB (*m/e*, based on ^{101}Ru): 1132 [M^+]. UV−vis data, λ_{max} (nm, ϵ(M^{-1} cm^{-1})): 770(6410), 476(15 000). ν(C≡C) (cm^{-1}, KBr disk): 2062(m), 1930(m). χ_g, 5.25 × 10^{-6} emu, μ_{eff}, 3.99 μ_B.

Data for **4b**: R_f, 0.38. Anal. Found (Calc)for $C_{58}H_{41}N_8Ru_2 \cdot C_6H_{14}$: C, 67.62 (67.75); H, 5.01 (4.99); N, 9.37 (9.72). MS-FAB (*m/e*, based on ^{101}Ru): 1052 [M^+]. UV−vis data, λ_{max} (nm, ϵ(M^{-1} cm^{-1})): 773(7350), 456(15 200). ν(C≡C) (cm^{-1}, KBr disk): 2072(w), 1943(w). χ_g, 4.92 × 10^{-6} emu, μ_{eff}, 3.73 μ_B.

Preparation of $Ru_2(ap)_4(C_{10}Ph)$ (5b). To a 50 mL THF solution containing 0.478 g of $Ru_2(ap)_4(C_6H)$ (**3c**) (0.50 mmol) was added 10.0 mL of 1.0 M $HC_2Si^iPr_3$ (THF), 0.10 mL of TMEDA, and 20 mg of CuCl. Air was gently bubbled through the solution, and the reaction was terminated upon the full consumption of **3c**. The reaction mixture was then filtered through a 2 cm sil-gel pad. The crude $Ru_2(ap)_4(C_8Si^iPr_3)$ was desilylated in situ by adding TBAF and stirred for 10 min. To the resultant solution of crude $Ru_2(ap)_4(C_8H)$ was immediately added 10.0 mL of 1.0 M HC_2Ph in THF, 0.10 mL of TMEDA, and 20 mg of CuCl, and air was gently bubbled through the solution. The reaction was complete in 30 min, as indicated by TLC. After the solvent removal, product **5b** was extracted from the residue using 100 mL of acetone. The crude extract was further purified by column chromatography using a linear gradient of eluents (hexanes/ethyl acetate/triethylamine, 95:0:5−85:10:5, v/v) to yield **5b** as a brown crystalline material (0.194 g, 36% based on **3c**).

Data for **5b**: R_f, 0.43. Anal. Found (Calc) for $C_{60}H_{41}N_8Ru_2 \cdot H_2O$: C, 65.51 (65.86); H, 4.02 (3.96); N, 10.20 (10.24). MS-FAB (*m/e*, based on ^{101}Ru): 1076 [M^+]. UV−vis data, λ_{max} (nm, ϵ(M^{-1} cm^{-1})): 775(7180), 475(17 200). ν(C≡C) (cm^{-1}, KBr disk): 2043(w), 1943(w). χ_g, 5.36 × 10^{-6} emu, μ_{eff}, 3.92 μ_B.

Crystal Data for 3c·H_2O. A single crystal of **3c** was grown via slow diffusion of methanol into a CH_2Cl_2 solution. M = 970.03 g/mol; tetragonal; space group $P4nc$, a = 10.3951(5) Å, c = 20.137(1) Å, V = 2176.0(2) $Å^3$; Z = 2; D_{calc} = 1.481 g/cm^3; μ = 0.742 mm^{-1}; F(000) = 982. Data were collected using a brown block of dimensions 0.36 × 0.17 × 0.10 mm^3 on a Bruker SMART1000 CCD-based X-ray diffractometer system using Mo Kα (λ = 0.71073 Å) at 300 K. Of 23 582 reflections (2.02° ≤ θ ≤ 34.98°) measured, 3962 were unique (R_{int} = 0.040). Least squares refinement based on 2741 reflections with $I \geq 2\sigma(I)$ and 145 parameters led to convergence with final R1 = 0.045 and wR2 = 0.105. Data collection and processing procedures were the same as previously described.[88]

(88) Xu, G.-L.; Campana, C.; Ren, T. *Inorg. Chem.* **2002**, *41*, 3521.

Scheme 5. Degenerate Four-Wave Mixing Apparatus for Investigation of $\chi^{(3)}$ Coefficients

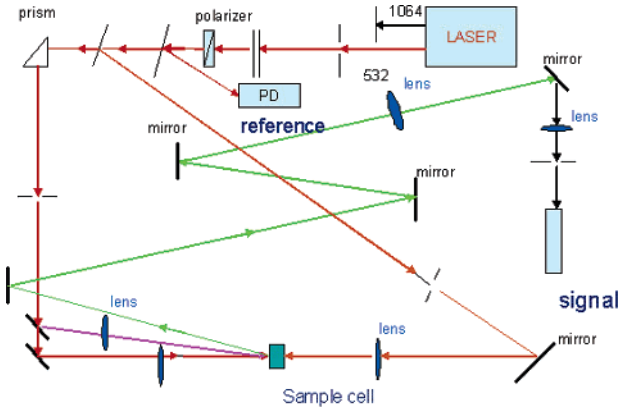

Nonlinear Optical Measurements. The $Ru_2(ap)_4(C_{2k}Ph)$ solutions were made in anhydrous toluene (ACROS with purity 99.8%). The diagram of the degenerate four-wave mixing DFWM apparatus is shown in Scheme 5. A frequency-doubled, Q-switched Nd:YAG laser with a temporal pulse width of 8 ns and a repetition rate of 10 Hz was used as the light source. The diameter of the laser beam was decreased to about 1.4 mm by an aperture; a combination of half-waveplate and Y-polarizing cube was used to attenuate the energy. One of the beam splitters was used to split the attenuated beam into two parts. The reflected beam was used to monitor the incident laser energy. The transmitted beam went to the second beam splitter that was used to split the beam into two parts: one is 30%, which became the B-pump, the other is 70%, which is split into two parts by the third beam splitter; the 25% beam became the probe beam and the 75% became the F-pump. Scheme 5 shows schematically the beam configurations used in the DFWM experiments. In this configuration, the forward and backward pump beams (F-pump and B-pump) nearly counterpropagate (NCP) as they impinge on the sample, the angle between them in the vertical plane being $\theta_B = 1.6°$. A third beam, the probe, is also incident on the sample at an angle to the F-pump in the horizontal plane of $\theta_p = 1.6°$. The angular separation between the F-pump and the B-pump causes the signal beam to propagate in a direction that is spatially distinct from the probe.[89] The three beams were temporally and spatially overlapped in the sample, which was contained in a 5 mm rotating quartz cuvette. The phase conjugate signal was detected with a silicon photodiode. Carbon disulfide (CS_2) was used as reference to calibrate the measurements in DFWM. The signal pulses are detected by a photomultiplier tube, and a computer-controlled neutral-density filter wheel is used to expand the detector dynamic range. In this case, the data can be fit to $I_s = qI_L^3$, where q is proportional to the product of the square of the path length, L, and the modulus of the third-order susceptibility, $\chi^{(3)}$, and is inversely proportional to the fourth power of the linear refractive index n_0. The sample susceptibility is obtained from the data using[90]

$$\left|\chi^3_{\text{sample}}\right| = \left|\chi^3_{\text{ref}}\right|\left(\frac{q_{\text{sample}}}{q_{\text{ref}}}\right)^{1/2}\left(\frac{n_{\text{sample}}}{n_{\text{ref}}}\right)^2\left(\frac{l_{\text{sample}}}{l_{\text{ref}}}\right)\left(\frac{\alpha l}{e^{-\alpha i/2}(1-e^{-\alpha l})}\right)$$

A value of n_{sample} at 532 nm is used for the neat solvent, following Martin's determination made by means of a Kramers−Kronig transformation of the absorption spectrum. In common with others,[91] we choose for the susceptibility of the CS2 reference the absolute value obtained by Xuan et al. using Jamin interferometry.[92] The actual value used is $\chi^{(3)}yyyy = 3.8 \times 10^{-20}$ m^2 V^{-2}, which is obtained by multiplying $\chi^{(3)}yyyy$, as reported by Xuan et al.[92]

The nonlinear transmission measurements were carried out at 800 nm using femtosecond laser pulses at the 800 nm beam, which was passed through a circular variable neutral density filter (CVNDF) in order to vary the input intensity. This beam is passed through a beam splitter, and the reflected beam is used as a reference beam, which is detected using the reference photodiode. The transmitted beam is passed through the 2 in. focal lens and is focused on the 1 mm quartz cell, and the intensity of the transmitted beam is measured using an OPHIR power meter. The ratio of output intensity to that of input intensity gives us the nonlinear transmission. A series of measurements are carried out for different input powers, and NLTs were plotted as a function of input intensity. Compounds $Ru(ap)_4(C_{2k}Ph)$ have a strong linear absorption at 800 nm. Thus, corrections to the linear absorption were also carried out during the analysis.

Acknowledgment. We gratefully acknowledge the financial support from the National Science Foundation (CHE-0242623 to T.R.; DMR-0134691 to T.G.G.) and the Army Research Office (41319-MS to T.G.G.).

Supporting Information Available: CV plots and vis−NIR spectra for compounds **2a**−**4a** (PDF) and X-ray crystallographic files in CIF format for the structure determination of compound **3c**. This material is available free of charge via the Internet at http://pubs.acs.org.

OM050171I

(89) Kuebler, S. M.; Denning, R. G.; Anderson, H. L. *J. Am. Chem. Soc.* **2000**, *122*, 339.

(90) Beddard, G. S.; McFadyen, G. G.; Reid, B. D.; Thorne, J. R. G. *Chem. Phys.* **1993**, *172*, 363.

(91) Cui, Y.; Zhao, M.; He, G. S.; Prasad, P. N. *J. Phys. Chem.* **1991**, *95*, 6842.

(92) Xuan, N. P.; Ferrier, J. L.; Gazenger, J.; Rivoire, G. *Opt. Commun.* **1984**, *51*, 433.